nature communications

Article

https://doi.org/10.1038/s41467-024-52552-7

Ultrathin near-infrared transmitting films enabled by deprotonation-induced intramolecular charge transfer of a dopant

Received: 13 November 2023

Accepted: 30 August 2024

Published online: 18 September 2024

Check for updates

Dingfang Hu, Lingya Peng, Wenjun Xu, Shenghui Zhang, Zhongshan Liu & Yu Fang

Near-infrared transparent films demonstrate important applications in many fields, but how to eliminate light interference from ultraviolet-visible region and how to tackle the trade-off effect between film thickness and transmittance remain as challenges. Herein, we report a near-infrared transparent film that achieves high-efficient combination of thin thickness (16 μm), suitable cut-off wavelength (890 nm), and ideal transmittance ($T_{NIR} > 90\%$, $T_{Vis} < 1\%$). Moreover, the film is photo-chemically stable, heating resistance and moisture insensitive. The key component of the film is a complex of a specially designed boron compound containing a perylene monoimide unit (PMI-CBN) with an organic base 1,8-diazabicyclo[5,4,0]undec-7-ene. The complex depicts red-shifted absorption from 709 to 943 nm owing to deprotonation of the N-H group of PMI-CBN. Dispersion of the complex in polymethyl methacrylate results in the high-performance film. As demos, the film is successfully used for night vision imaging and information encryption.

Visibly opaque but near-infrared (NIR) transparent materials have strong absorption in the visible region but high transparency in the near-infrared domain. This kind of material demonstrates potential applications in security imaging, optical detection, night vision imaging, forensic application, anti-counterfeiting, etc.[1–4]. Till today, the prevalent NIR transparent materials are inorganics, such as metal oxides, silicon-based semiconductors, and chalcogenide glasses. These materials, however, are inflexible and even brittle, which makes them hard to be processed and applicated in newly emerged flexible and wearable devices[5–8].

Recently, organic molecules have been developed to produce NIR transparent films by controlling aggregation states of dyes[9,10], and by constructing organic charge-transfer complexes in polymeric films[11,12]. Compared to inorganic materials, organic NIR transparent materials have merits of flexibility, tunable optical transmittance, and remarkable solution-processible properties, but the types of the materials are very limited[13–16]. To produce NIR transparent filters, most absorbers need to be blended with polymers, whether they are inorganics or organics. A consequent issue is the trade-off effect between absorber-doping-induced film thickness and transmittance. For example, increasing the absorber content in a NIR transparent film generally shifts the cut-off wavelength to the NIR region and inhibits transmittance in the visible region but unavoidably leads to the decay of transmittance in the NIR region, as well as an increase in film thickness. This is why the thicknesses of qualified NIR transparent films reported till today range from hundreds of micrometers to several millimeters, making it difficult to minimize devices relevant to NIR transparent films[11,17,18].

An additional shortcoming of organic NIR transparent materials is narrow absorption that makes it difficult to eliminate light interference throughout ultraviolet–visible (UV–vis) region[19–21]. To broaden absorption spectra to 780 nm and beyond, the general strategies adopted are to extend the π-conjugated skeletons of the dyes[22–24] and produce radical anions[25–27]. Modulation of the π-conjugated molecules, however, requires tedious synthesis, and utilization of the radical anions encounters poor stability. Therefore, new strategies are needed to develop high-quality visible opaque but NIR transparent organic materials.

We previously reported a four-coordinated boron compound with an imine group (N–H), whose absorption band remarkably shifted

Key Laboratory of Applied Surface and Colloid Chemistry of Ministry of Education, School of Chemistry and Chemical Engineering, Shaanxi Normal University, Xi'an 710119, P. R. China. e-mail: zhongshan.liu@snnu.edu.cn; yfang@snnu.edu.cn

https://doi.org/10.1038/s41467-024-52552-7

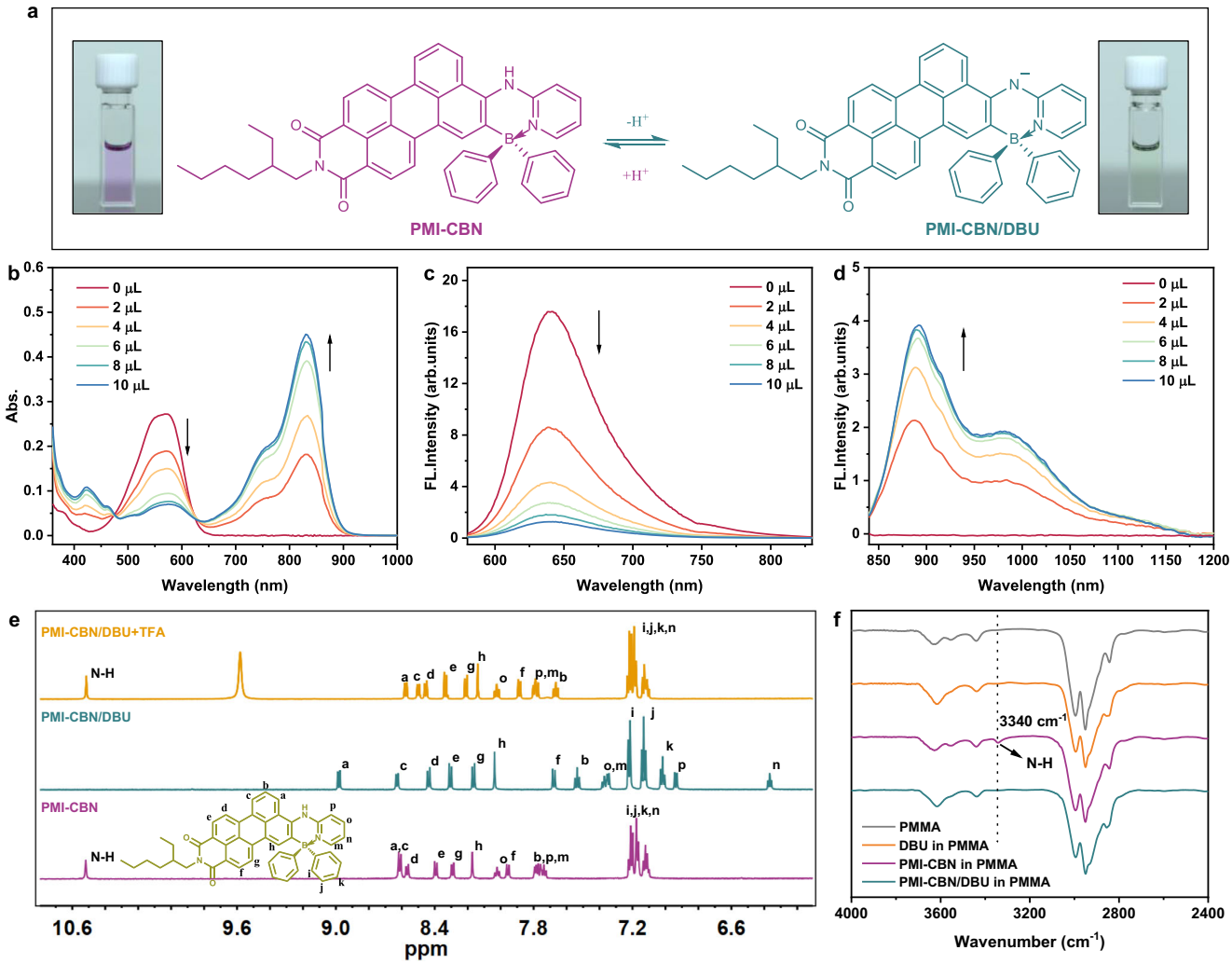

Fig. 1 | Deprotonation process of PMI-CBN compound. a Chemical structure of PMI-CBN and PMI-CBN/DBU. Inset: Photographs of the corresponding solutions under natural light. **b**–**d** Absorption and fluorescence emission spectra of the tetrahydrofuran solution of PMI-CBN (5×10^{-6} mol L^{-1}) with the addition of DBU, where the excitation wavelengths for the spectra shown in (**c**, **d**) are 570 and 830 nm, respectively. **e** ^{1}H NMR spectra of PMI-CBN, and PMI-CBN/DBU before and after adding TFA in DMSO-d_6. **f** FT-IR spectra of the polymethyl methacrylate (PMMA) film, as well as the PMMA films doped with DBU, PMI-CBN, or PMI-CBN/DBU.

from 420 to 580 nm under stimulation with tetrabutylammonium fluoride (TBAF)[28]. It is confirmed that such red-shift is derived from enhanced intramolecular charge transfer (ICT) of the compound owing to deprotonation of its N–H group. Inspired by the observation, we attempt a combination of deprotonation and extension of the π-conjugated unit to develop a high-performance organic NIR transparent material. As shown in Fig. 1a, a perylene monoimide (PMI) unit was introduced to synthesize a *C,N*-chelate boron compound (PMI-CBN). The combination of the compound with an organic base, 1,8-diazabicyclo[5,4,0]undec-7-ene (DBU), resulted in an absorption far-red shifted PMI-CBN/DBU complex. Doping the PMI-CBN/DBU complex in a polymethyl methacrylate (PMMA) film produced a thin and flexible NIR transparent film, which was further used for night vision imaging and information security.

Results

Synthesis and characterization of PMI-CBN and PMI-CBN/DBU complex

In previous studies, we developed a protocol for synthesizing a four-coordinated boron compound with 1,8-naphthalimide as an electron-accepting unit[28]. We found that deprotonation of the imine group (-NH-) in the compound enhances the ICT process, which induces red-shifted absorption. However, the absorption bands of the systems are still in the visible region (580 nm). To move the cut-off wavelength to the NIR region, we synthesized a four-coordinated boron compound PMI-CBN by introducing a larger π-conjugated moiety that is perylene monoimide (Supplementary Fig. 1). Detailed synthesis procedures and characterization data are provided in the Supplementary Information. The UV–vis absorption spectra of PMI-CBN in solvents with varied polarities are depicted in Supplementary Fig. 2. As seen, the absorption spectrum of PMI-CBN shows distinct 0–0 and 0–1 vibronic bands in toluene, but the fine structure loses with increasing solvent polarity, probably owing to enhanced dye-solvent interaction.

Owing to the strong proton-donating capability of the N–H group, PMI-CBN, as prepared, can undergo deprotonation in response to the addition of a suitable base. For instance, the introduction of DBU, a typical organic base, resulted in an ionic complex denoted as PMI-CBN/DBU, which is accompanied by remarkable red-shift of the absorption and fluorescence emission of the system (Fig. 1a). As depicted in Fig. 1b, the absorption peak of PMI-CBN in THF appeared at ~573 nm and upon successive addition of DBU, the absorption gradually diminished, followed by the appearance of a new absorption centered at ~832 nm. Concurrently, the solution color changed from purple to pale green (Fig. 1a). Other organic bases, such as TBAF and tetrabutylammonium hydroxide (TBAH), showed a similar effect upon the absorption and emission of PMI-CBN (Supplementary Fig. 3). Interestingly, addition of

trifluoroacetic acid (TFA) to the organic base treated PMI-CBN solution led to the reappearance of the original PMI-CBN absorption while the absorption at longer wavelengths disappeared. Figure 1c, d shows the fluorescence emission spectra of PMI-CBN and PMI-CBN/DBU in THF. As seen, the fluorescence emission of PMI-CBN centering at 640 nm decreased with increasing DBU content, but a new emission appeared within the NIR range (840–1200 nm). The newly appeared and remarkably red-shifted absorption and emission must originate from the formed PMI-CBN/DBU complex. The red-shifted absorption and fluorescence emission could be ascribed to the enhanced ICT effect compared to the neutral state as known from theoretical calculations (Supplementary Tables 1 and 2 and Supplementary Fig. 4).

To confirm the presence of the deprotonated nitrogen anion in PMI-CBN/DBU, the ^{1}H NMR spectra of PMI-CBN, PMI-CBN/DBU, and PMI-CBN/DBU with TFA in DMSO-d_6 were recorded. The results are shown in Fig. 1e and Supplementary Fig. 5, where the N–H proton signal (10.52 ppm) of PMI-CBN completely vanished after adding DBU. The proton signals, excepting Ha, shifted toward a higher field owing to increased electron density in the PMI-CBN moiety due to deprotonation of the N–H group. The lower field shift of the Ha signal could be a result of enhanced intramolecular hydrogen bonding also probably due to deprotonation of the N–H group. The N–H signal at 10.52 ppm reappeared, and the Ha signal shifted to the original position with the addition of TFA, indicating the re-formation of the N–H group. The improved resolution of certain proton signals could be attributed to the change in the solvent environment. The COSY spectra shown in Supplementary Figs. 6, 7 also confirmed the deprotonation process. We further measured the electrical conductivity of the PMI-CBN/DBU solution (Supplementary Fig. 8). As observed, the electrical conductivities of PMI-CBN and DBU in *N,N*-dimethylformamide (DMF) are 5.3 μS/cm and 5.1 μS/cm, respectively. Upon mixing the two solutions, however, the electrical conductivity significantly increased to 29.2 μS/cm, indicating the generation of charged species. FT-IR spectroscopy measurements were further made to prove deprotonation of PMI-CBN/DBU in the film state (Fig. 1f). The stretching absorption at ~3340 cm^{-1} of the N–H group of PMI-CBN in the film state disappeared in the PMI-CBN/DBU/PMMA film, which confirmed not only deprotonation but also stability of the complex in the solid state.

NIR transparent Performance of PMI-CBN/DBU/PMMA Film

Encouraged by the tunable broadband absorption of the PMI-CBN/DBU complex in solutions, we explored its optical properties in the film state. PMMA is a prevalent polymer matrix for the construction of functional films because of its exceptional optical transmittance and numerous advantages, such as lightweight, corrosion-resistant, and good processibility. Accordingly, we prepared a visibly opaque but NIR transparent film by incorporating the PMI-CBN/DBU complex as found in the solution state into a PMMA matrix. The preparation process is schematically depicted in Fig. 2a. Briefly, a certain amount of the PMI-CBN/DBU solution was mixed with a given amount of the DMF solution of PMMA. The mixture was drop-casted onto a quartz substrate, then the solvent was evaporated at 100 °C, and then a self-standing PMI-CBN/DBU/PMMA film was obtained. Similarly, a PMI-CBN/PMMA film as a control was also prepared. As illustrated in Fig. 2b, the PMI-CBN/DBU/PMMA film exhibits a pronounced red shift compared to the PMI-CBN/PMMA film in absorption spectra. The absorption edge is extended from 709 to 943 nm. We then examined the transmittance of the two films over UV–vis–NIR light range (Fig. 2c). As seen, the PMI-CBN/DBU/PMMA film features a visibly opaque but NIR transparent property while the PMI-CBN/PMMA film fails to block visible light. The difference between the two films can be clearly seen in the photographs of them (Fig. 2d), where the PMI-CBN/DBU/PMMA film is much more-blacker and smoother. The PMI-CBN/DBU complex plays a key role in the transmittance property of the PMI-CBN/DBU/PMMA film. We measured the molar absorption coefficient of the PMI-CBN/DBU complex in film state, and it was revealed to be 5.75×10^4 L mol^{-1} cm^{-1}, which is in accordance with the result from solution measurement (5.67×10^4 L mol^{-1} cm^{-1}, Supplementary Figs. 9, 10).

An ideal NIR transparent film should show transmittance below 2% in the visible region and higher than 60% in the NIR region[13]. Based on this criterion, we investigated the influence of the molar ratio of PMI-CBN to DBU and PMI-CBN/DBU contents in films on their optical properties, respectively. Supplementary Fig. 11 shows that when the molar ratio of DBU to PMI-CBN is below 5, where PMI-CBN to PMMA was kept at 0.62 mg/3.5 mg, the film is unable to fully block the transmission of visible light. This limitation is primarily attributed to the solidification property of the PMMA matrix, which hinders the effective contact between PMI-CBN and DBU molecules. To achieve optimal visible light blocking, an excessive organic base needs to be used. The ultimately determined molar ratio of PMI-CBN to DBU is 1:5.

We further optimized the doping content of PMI-CBN absorber in the PMI-CBN/DBU/PMMA films. Figure 2e shows that with increasing the doping content of PMI-CBN absorber from 0 to 9.5 wt%, the transmittance of visible light decreased to as low as 1%, while the transmittance of NIR radiation remained except for slight red-shifts at cut-off wavelength positions. Further increasing PMI-CBN absorber content in films showed ignorable changes in transmittance spectra. To clearly demonstrate these changes, Fig. 2f shows the plots of the transmittances at 480 and 1200 nm of the films with different doping ratios. Figure 2g shows the photographs of the PMI-CBN/DBU/PMMA films of different doping ratios. With increasing PMI-CBN absorber contents, the color of the as-prepared films changed from green to black, and the Chinese characters behind the films became gradually obscured owing to increased blocking of visible light. We also studied the film thickness effect on transmittance (Supplementary Figs. 12–15). Under the condition of constant PMI-CBN volume, the film thickness can be effectively adjusted by precisely controlling the amount of PMMA added, while maintaining its light transmittance unaffected. To achieve the film that can completely block visible light while possessing ultrathin properties to meet the application requirements of wearable devices, for the given size of the substrate, 40 μL of the PMMA solution (12.9 wt% of PMI-CBN absorber) is enough to produce a qualified PMI-CBN/DBU/PMMA film (16 μm).

To be usable in flexible electronics and wearable devices, the NIR transparent film should be flexible, stable, and uniform, and thereby we examined the relevant properties of the PMI-CBN/DBU/PMMA film as fabricated. As shown in Fig. 3a, b, the PMI-CBN/DBU/PMMA film is self-standing and flexible. General bending shows no observable damage to its structure. Cross-sectional scanning electron microscope (SEM) studies revealed that the PMI-CBN/DBU/PMMA film is uniform, and the thickness is about 16 μm (Fig. 3c). Further energy dispersive X-ray (EDX) mapping studies demonstrated that the relevant elements of C, N, O, and B are uniformly dispersed throughout the whole film (Fig. 3d), indicating uniform dispersing of PMI-CBN/DBU within the PMMA matrix. The fact that the transmittance spectra over the UV–vis–NIR region recorded at three randomly selected positions on the film are almost the same also confirms the uniformness of the NIR transparent film (Supplementary Fig. 16). These results indicate that the PMI-CBN/DBU/PMMA film as prepared is both microscopically and macroscopically uniform, which could be benefited from the good solubility of the PMI-CBN/DBU complex in the solvent and the compatibility of the complex with the PMMA matrix. The water contact angle of the as-prepared film is 84.7°, suggesting a certain degree of hydrophilicity (Fig. 3e and Supplementary Movie 1). It is the not-too-high hydrophilicity that may explain why the film is moisture-resistant, where up to 8 h exposure to a humid environment with a relative humidity of 90% showed no observable effect upon its optical property (Fig. 3f). Furthermore, the PMI-CBN/DBU/PMMA film is also photochemically and thermally stable as seven days respective storage in the environment of −20 °C and 100 °C showed no significant effect upon the transmittance spectra of the examined films (Fig. 3g, h). The thermo-stability of the

https://doi.org/10.1038/s41467-024-52552-7

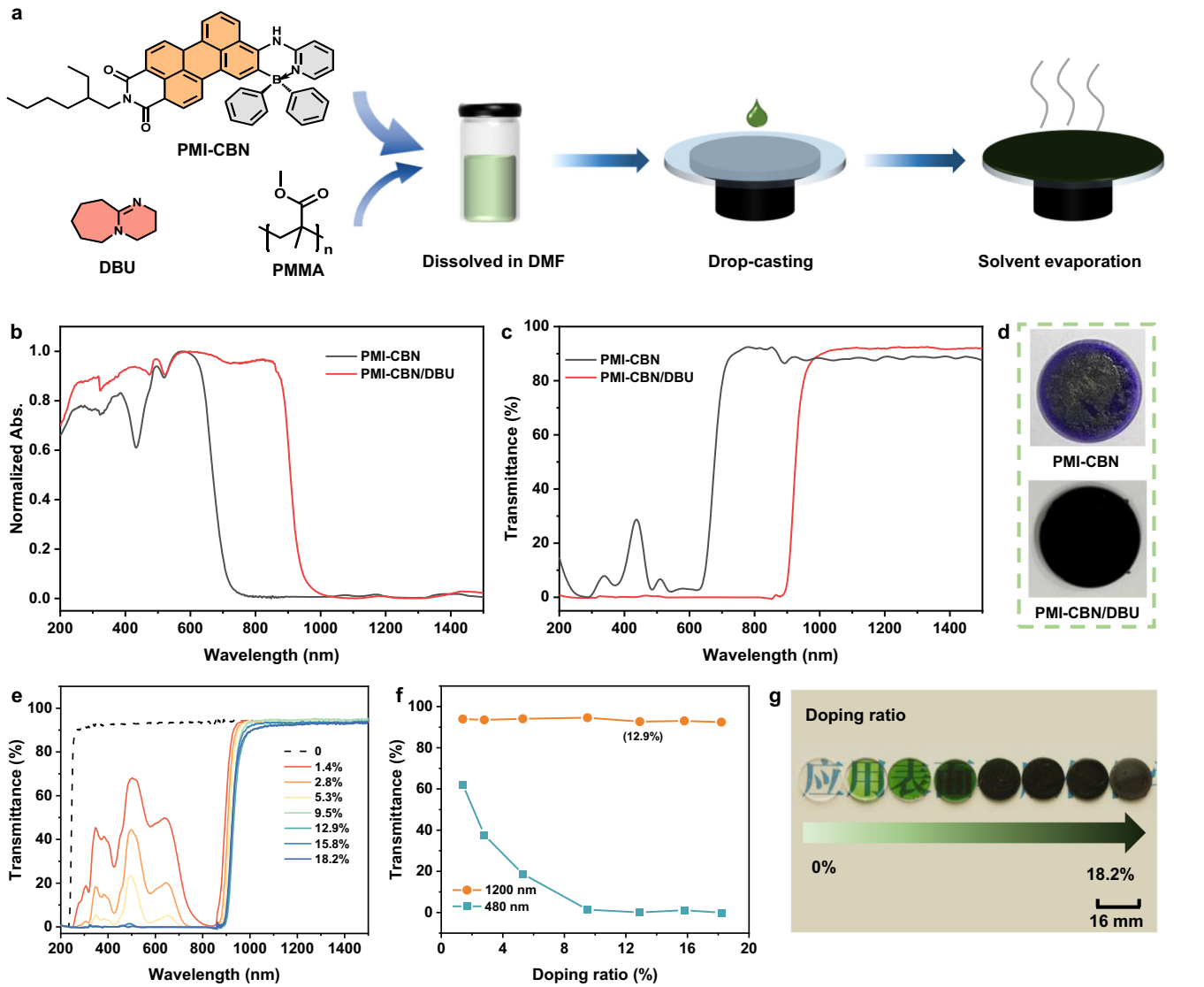

Fig. 2 | Preparation and optical properties of NIR transparent film. a Schematic representation of the preparation of the PMMA films of PMI-CBN/DBU. **b**, **c** UV–vis–NIR absorption and transmittance spectra of the PMMA films of PMI-CBN and PMI-CBN/DBU. **d** Photographs of the two films as prepared. **e** Transmittance spectra of the PMI-CBN/DBU/PMMA films with varying doping ratios of PMI-CBN absorber. **f** Plots of the transmittances recorded at 480 and 1200 nm versus PMI-CBN absorber doping ratios. **g** Photographs of the PMI-CBN/DBU/PMMA films with doping contents varied from 0 to 18.2 wt%.

films was further examined using the thermogravimetric analysis (TG) technique, which revealed that there was no significant weight loss below 130 °C (Supplementary Fig. 17), and the doped DBU only started to significantly escape from the film when the temperature exceeds 130 °C. Moreover, the DBU content, as determined, is about 12.1 wt%, which is close to the theoretical value of 14.2 wt%.

We compared our PMI-CBN/DBU/PMMA film to other reported organic NIR transparent films (Table 1). Clearly, our film achieved an excellent combination of thickness (16 μm), cut-off wavelength (890 nm), and transmittance (>90% in the NIR region, <1% in the visible region). Moreover, our film also shows a sharper edge slope at the cut-off wavelength position, which can accurately eliminate interference from the light source.

Applications for night vision imaging and information security

Night vision imaging technology plays an important role in the field of vehicle driving and monitoring as it can be used to identify objects in the dark or hazy weather[29]. The filters with good NIR transparency are essential components of the technology. Taking advantage of the prominent transmittance of the PMI-CBN/DBU/PMMA film to NIR radiation, we investigated its application in night vision photography. To conduct the test, a routine smartphone was modified. Specifically, the built-in NIR reflector of the lens in the smartphone was removed, and our PMI-CBN/DBU/PMMA film was attached to the top of the lens (Supplementary Fig. 18). Then, the modified smartphone was used for night surveillance. As shown in Fig. 4a, a routine smartphone can capture the image of the plant under natural light, but it fails in a dark environment. Instead, the modified smartphone is able to take a picture of the plant under the dark environment provided a NIR light source (1050 nm) is used.

We further demonstrated an application of our NIR transparent film for information security. A proof-of-concept experiment was conducted using the PMI-CBN/DBU/PMMA film. As depicted in Fig. 4b, we employed red, green, blue, and black colors to print the phrase 'Fang Group'. A NIR reflective filter was placed over the letter 'G'. When images were taken with a smartphone lacking the PMI-CBN/DBU/PMMA film, all letters were clearly visible. However, photographs taken with the smartphone equipped with the PMI-CBN/DBU/PMMA film displayed a different outcome. Due to the inability to transmit visible light of this film, letters printed in red, green, and blue colors were

https://doi.org/10.1038/s41467-024-52552-7

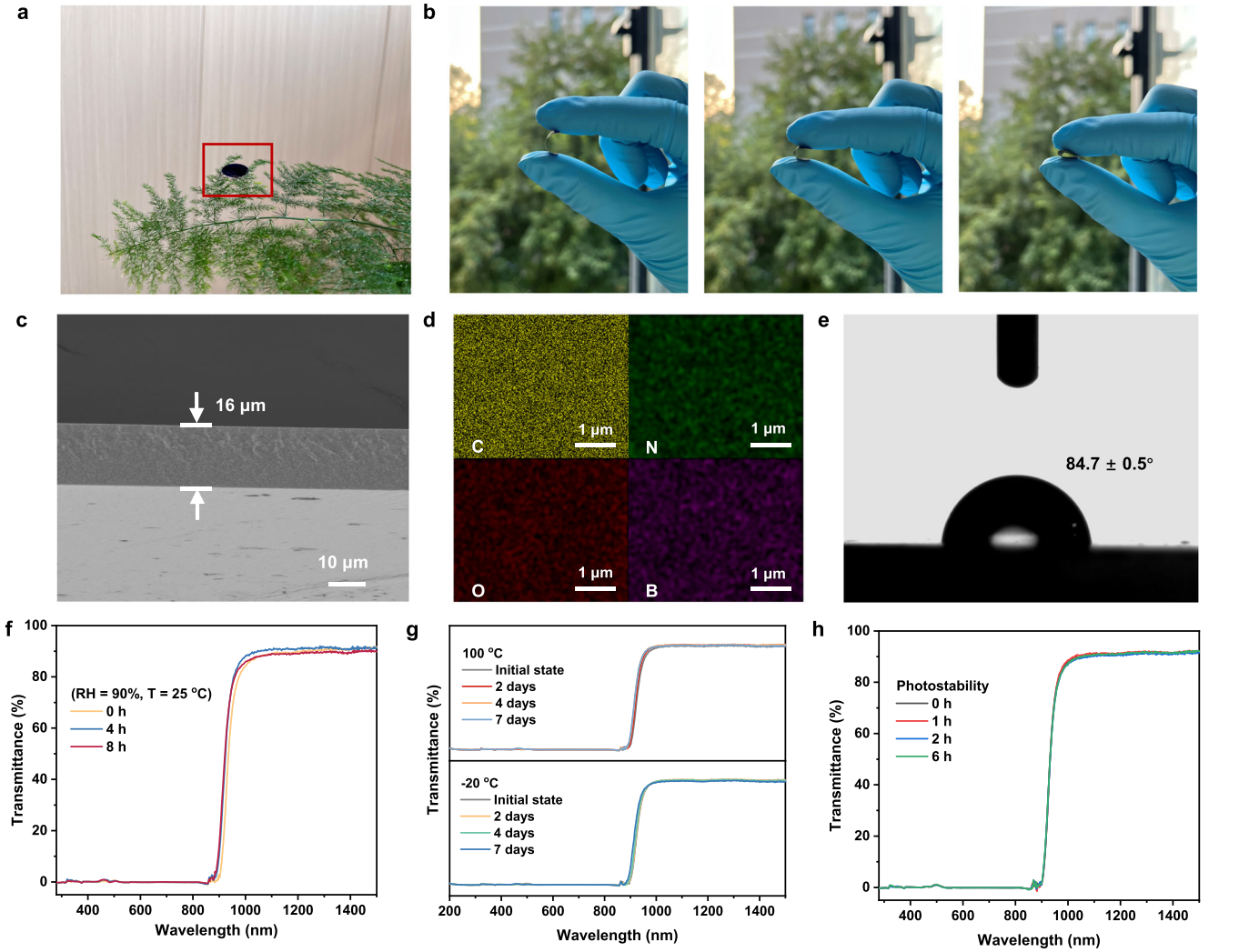

Fig. 3 | Flexibility, uniformity, and stability tests for NIR transparent film. **a** Photograph of the self-standing PMI-CBN/DBU/PMMA film. **b** PMI-CBN/DBU/PMMA film of different bending angles. **c** Cross-sectional SEM image of the PMI-CBN/DBU/PMMA films. **d** EDX mapping images of the PMI-CBN/DBU/PMMA films, where the capital letters of C, N, O, and B represent carbon, nitrogen, oxygen, and boron elements, respectively. **e** Water contact angle test for the PMI-CBN/DBU/PMMA film. **f** and **g** Humidity and temperature stability of the PMI-CBN/DBU/PMMA film. **h** Photo-stability of the PMI-CBN/DBU/PMMA film under 1 kW m^{-2} illumination. The PMI-CBN/DBU/PMMA film is prepared with 12.9 wt% doping content of the PMI-CBN absorber.

Table 1 | Comparison between our film and reported organic NIR transparent films

Material	Cut-off wavelength	T_{Vis}	T_{NIR}	Thickness	Absorber content	Polymer matrix	References
DPP-Amide[a]	850 nm	<1%	~70%	1.46 mm	0.15 wt%	PDMS[d]	9
PNCs/SQ[b]	742 nm	<2%	>80%	425 nm	1.2 wt%	–	13
TTF-TCNB[c]	1055 nm	<2%	~80%	400 μm	20 wt%	PMMA	11
PMI-CBN/DBU	890 nm	<1%	>90%	~16 μm	12.9 wt%	PMMA	This work

a diketopyrrolopyrrole-Amide; **b** perovskite nanocrystals/squaraine; **c** tetrathiafulvalene-1,2,4,5-tetracyanobenzene; **d** poly(dimethylsiloxane); Optical transmittance in the visible (T_{Vis}) and near-infrared (T_{NIR}) region.

indiscernible. As expected, the letter 'G' covered by a NIR reflective filter cannot be detected. As illustrated in Fig. 4c and Supplementary Movie 2, a quick response (QR) code was printed on paper, and then covered with a black PMI-CBN/DBU/PMMA film. Under daylight condition, the image of the QR code beneath the black film was concealed. When a modified smartphone with NIR sensitivity was used, the hidden QR code can be clearly extracted (IR light source, 1050 nm). In this way, information stored in the QR code can be concealed. Of course, access of the information needs a specially designed code-scanning machine such as the PMI-CBN/DBU/PMMA film modified smartphone.

Discussion

In summary, we demonstrated a PMI-CBN/DBU complex and relevant construction of a visibly opaque but NIR transparent film. The deprotonation-induced ICT effect and a larger π-conjugated unit in the complex endowed the PMI-CBN/DBU/PMMA film as-prepared with transmittance below 1% in visible region but higher than 90% in NIR region. Compared to documented organic NIR transparent films, our PMI-CBN/DBU/PMMA film achieved a high-efficient combination of thickness, cut-off wavelength, and transmittance. Taking advantages of flexibility, self-standing, light weight, stability and unique optical

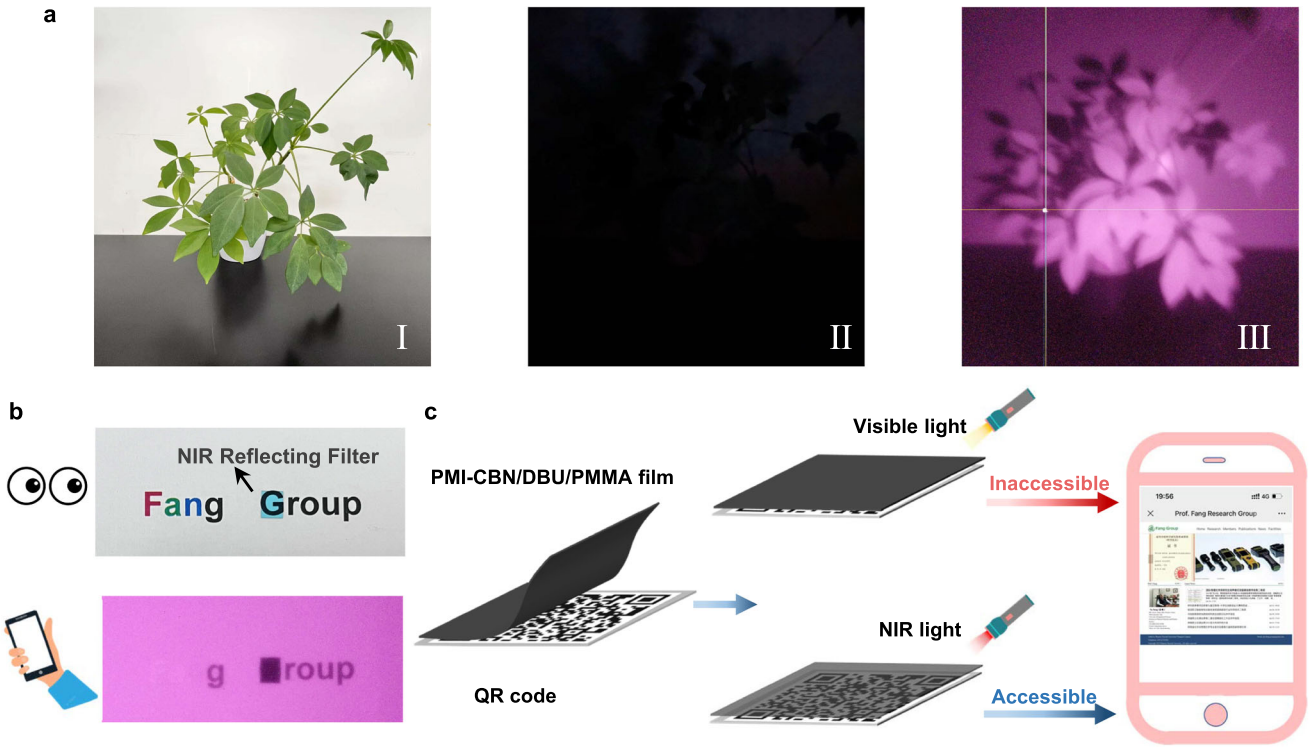

Fig. 4 | Applications for night vision imaging and information security. **a** Photographs taken with (I) a normal smartphone under daylight, (II) a normal smartphone in the dark, (III) a smartphone equipped with the PMI-CBN/DBU/PMMA film in the dark (NIR source, 1050 nm). **b** Photograph of the printed words captured by the smartphone without/with PMI-CBN/DBU/PMMA film, where "F, a, n" were printed in red, green and blue inks, respectively, while the "g, Group" printed in black ink. *Note*: The letter "G" was covered with a NIR reflecting filter. **c** Reading information from a hidden QR code.

properties, the NIR transparent film developed this work may find important applications in NIR imaging, information encryption, flexible electronics, wearable devices, etc.

Methods

Materials

Perylene-3,4,9,10-tetracarboxylic dianhydride (Bidepharm), 2-ethylhexylamine (Titan), potassium aryltrifluoroborates (Bidepharm), $Zn(OAc)_2{\cdot}2H_2O$ (Titan), imidazole (Titan), $Na_2S_2O_3$ (National Pharmaceutical Reagent Co., China), Br_2 (National Pharmaceutical Reagent Co., China), 2-aminopyridine (Macklin), NaO*t*-Bu (Macklin), $SiCl_4$ (Macklin), $Pd_2(dba)_3$ (Adamas), P(*t*-Bu)$_3$ (TCI), *i*-Pr_2NEt (Adamas) and 1,8-diazabicyclo[5.4.0]-7-undecene (Adamas) were obtained commercially. All solvents with analytical grade were purchased from National Pharmaceutical Reagent Co., China. Organic solvents used for the synthesis and spectroscopic measurements were freshly distilled. Water used for the synthesis was from a Milli-Q system. Column chromatography was performed with 200-300 mesh silica gel. All moisture and oxygen sensitive reactions were carried out under dry and nitrogen atmosphere.

Instrumentations

All ^{1}H NMR spectra were obtained on a Bruker Avance 600 NMR spectrometer using TMS as internal standard. Matrix-assisted laser desorption ionization time-of-flight (MALDI-TOF) mass spectrum was acquired on a Bruker maxis MALDI-TOF mass spectrometer. High-resolution mass spectra (HRMS) were recorded on the Bruker maxis UHR-TOF mass spectrometer with an APCI positive mode. UV−vis−NIR absorption and transmittance spectra were obtained on a Perkin-Elmer Lambd 1050 spectrophotometer at room temperature. Steady-state fluorescence emission spectra were acquired on a HORIBA Fluorolog-QM fluorescence spectrometer with xenon lamp as the light source. The morphology and thickness of the films were characterized using field emission scanning electron microscope (SU8220, Hitachi) and tabletop scanning electron microscope (TM3030, Hitachi), respectively. The water contact angles were observed by a video-based contact angle measuring device (OCA20, Dataphysics). The thermogravimetric analysis was performed on SDT-Q600 under nitrogen atmosphere. The electrical conductivity was measured on the conductivity meter (S400-K, Mettler Toledo). All optical images depicted in the paper were taken by a Canon 70D camera and a smartphone.

Preparation of PMI-CBN/DBU/PMMA Films

PMI-CBN (3.45 mg, 0.005 mmol) was dissolved in 1.0 mL of DMF, followed by adding 3.8 μL of DBU (3.8 mg, 0.025 mmol). This mixture was ultrasonicated for 5 minutes to obtain a homogenous PMI-CBN + DBU solution (molar ratio, PMI-CBN:DBU = 1:5). PMMA (100 mg) was dispersed in 1.0 mL of DMF and dissolved by heating (ρ = 950 mg mL^{-1}, ω_{PMMA} = 0.093). For preparation of the PMI-CBN/DBU/PMMA films, the PMI-CBN + DBU solution was mixed with the PMMA solution, and the resulting solutions were dropped onto a quartz substrate. After drying at 100 °C for 5 h, a series of self-standing PMI-CBN/DBU/PMMA films were obtained by varying doping ratios of PMI-CBN absorber in the PMMA matrix. For example, a film containing 12.9 wt.% PMI-CBN was prepared by mixing 180 μL of the PMI-CBN + DBU solution with 40 μL of the PMMA solution. The doping ratio of PMI-CBN absorber was calculated using formula, doping ratio = $\frac{m_{PMI-CBN}}{m_{PMI-CBN} + m_{DBU} + m_{PMMA}}$, where $m_{PMI-CBN}$, m_{DBU}, m_{PMMA} represent the weights of PMI-CBN, DBU, and PMMA in the solutions used for fabricating the films, respectively.

Data availability

The data that support the findings of this study are available within the article and the supplementary material. Source data are provided with this paper.

References

1. Lee, M. et al. Long-wave infrared transparent sulfur polymers enabled by symmetric thiol cross-linker. *Nat. Commun.* **14**, 2866 (2023).
2. Tonkin, S. J. et al. Thermal imaging and clandestine surveillance using low-cost polymers with long-wave infrared transparency. *Adv. Optical Mater.* **11**, 2300058 (2023).
3. Ji, C. G. et al. Decorative near-infrared transmission filters featuring high-efficiency and angular-insensitivity employing 1D photonic crystals. *Nano Res.* **12**, 543–548 (2019).
4. Tong, J. K. et al. Infrared-transparent visible-opaque fabrics for wearable personal thermal management. *ACS Photonics* **2**, 769–778 (2015).
5. Calvez, L., Ma, H.-L., Lucas, J. & Zhang, X.-H. Selenium-based glasses and glass ceramics transmitting light from the visible to the far-IR. *Adv. Mater.* **19**, 129–132 (2007).
6. Hwang, J. H. et al. A microphase separation strategy for the infrared transparency-thermomechanical property conundrum in sulfur-rich copolymers. *Adv. Optical Mater.* **11**, 2202432 (2023).
7. Zhang, X. H., Bureau, B., Lucas, P., Boussard-Pledel, C. & Lucas, J. Glasses for seeing beyond visible. *Chem. Eur. J.* **14**, 432–442 (2008).
8. Li, Y. et al. 2D $Ti_3C_2T_x$ MXenes: visible black but infrared white materials. *Adv. Mater.* **33**, 2103054 (2021).
9. Ghosh, S., Cherumukkil, S., Suresh, C. H. & Ajayaghosh, A. A supramolecular nanocomposite as a near-infrared transmitting optical filter for security and forensic applications. *Adv. Mater.* **29**, 1703783 (2017).
10. Praveen, V. K., Vedhanarayanan, B., Mal, A., Mishra, R. K. & Ajayaghosh, A. Self-assembled extended π-systems for sensing and security applications. *Acc. Chem. Res.* **53**, 496–507 (2020).
11. Tian, S. et al. Harnessing polymer-matrix-mediated manipulation of intermolecular charge-transfer for near-infrared security applications. *Adv. Mater.* **34**, 2204749 (2022).
12. Liao, Z. X., Miao, J. H., Liu, J. & Wang, L. X. All-fused-ring molecules with high photostability for near-infrared security and anti-counterfeiting applications. *Sci. China Mater.* **66**, 4037 (2023).
13. Muthu, C., Pious, J. K., Seethal, P. S., Krishna, N. & Vijayakumar, C. Formamidinium lead iodide perovskite nanocrystal/squaraine dye composite based visibly opaque and near-infrared transmitting material. *Adv. Optical Mater.* **8**, 2001130 (2020).
14. Zhang, J. et al. All-organic polymeric materials with high refractive index and excellent transparency. *Nat. Commun.* **14**, 3524 (2023).
15. Yu, D. X. et al. Thermochromic Ni(II) organometallics with high optical transparency and low phase-transition temperature for energy-saving smart windows. *Small* **19**, 2205833 (2023).
16. Kim, J. H. et al. An efficient narrowband near-infrared at 1040 nm organic photodetector realized by intermolecular charge transfer mediated coupling based on a squaraine dye. *Adv. Mater.* **33**, 2100582 (2021).
17. Griebel, J. J. et al. New infrared transmitting material via inverse vulcanization of elemental sulfur to prepare high refractive index polymers. *Adv. Mater.* **26**, 3014–3018 (2014).
18. Sisken, L. et al. Infrared glass-ceramics with multidispersion and gradient refractive index attributes. *Adv. Funct. Mater.* **29**, 1902217 (2019).
19. Min, Y., Cao, X., Tian, H. K., Liu, J. & Wang, L. X. B←N-incorporated dibenzo-azaacene with selective near-infrared absorption and visible transparency. *Chem. Eur. J.* **27**, 2065–2071 (2021).
20. He, Q. et al. Ultra-narrowband near-infrared responsive J-aggregates of fused quinoidal tetracyanoindacenodithiophene. *Adv. Mater.* **35**, 2209800 (2023).
21. Qi, Q. K. et al. Force-induced near-infrared chromism of mechanophore-linked polymers. *J. Am. Chem. Soc.* **143**, 17337–17343 (2021).
22. Xie, J. J. et al. A NIR dye with high-performance n-type semiconducting properties. *Chem. Sci.* **7**, 499–504 (2016).
23. Jiang, Y. et al. Fused isoindigo ribbons with absorption bands reaching near-infrared. *Angew. Chem. Int. Ed.* **57**, 10283–10287 (2018).
24. Kohl, C., Becker, S. & Müllen, K. Bis(rylenedicarboximide)-a,d-1,5-diaminoanthraquinones as unique infrared absorbing dyes. *Chem. Commun.* **23**, 2778–2779 (2002).
25. Zhang, A. D., Jiang, W. & Wang, Z. H. Fulvalene-embedded perylene diimide and its stable radical anion. *Angew. Chem. Int. Ed.* **59**, 752–757 (2020).
26. Wang, Z. L. et al. A persistent radical anion derived from a propeller-shaped perylene bisimide-carbazole pentad. *Chem. Commun.* **58**, 7082–7085 (2022).
27. Tang, B. H. et al. A supramolecular radical dimer: high-efficiency NIR-II photothermal conversion and therapy. *Angew. Chem. Int. Ed.* **58**, 15526–15531 (2019).
28. Hu, D. F. et al. A mild-stimuli-responsive fluorescent molecular system enables multilevel anti-counterfeiting and highly adaptable temperature monitoring. *Adv. Funct. Mater.* **32**, 2207895 (2022).
29. Bao, F. L. et al. Heat-assisted detection and ranging. *Nature* **619**, 743–748 (2023).

Acknowledgements

The authors acknowledge financial support from the National Key Research and Development Program of China (2022YFA1205502), the National Natural Science Foundation of China (21820102005, 22132002), the 111 project (B14041) and the Earmarked Fund of Shaanxi Province to Y. F. for this work.

Author contributions

Y. F., Z. L. and D. H. conceived the research project. Y. F. and Z. L. supervised the research work and wrote the paper. D. H. synthesized the PMI-CBN, and prepared NIR transmitting film and helped analyzing the data and writing manuscript. L. P. performed quantum chemical DFT calculations and analyzed the data. W. X. and S. Z. helped to performed the spectrum measurements. All authors contributed to the interpretation of the results, and have given approval to the final version of the manuscript.

Competing interests

The authors declare no competing interests.

Additional information

Supplementary information The online version contains supplementary material available at https://doi.org/10.1038/s41467-024-52552-7.

Correspondence and requests for materials should be addressed to Zhongshan Liu or Yu Fang.

Peer review information *Nature Communications* thanks Bo-Tau Liu, Yu-Che Lin, Huahua Huang and the other, anonymous, reviewer(s) for their contribution to the peer review of this work. A peer review file is available.